Computational Energy Science

Vol. 2, No. 2, p. 68-84, 2025

Original article

A productivity model for multi-thermal fluid huff-n-puff in horizontal wells: Application to heavy oil reservoirs

Xiuchao Jiang[1], Xiaohu Dong[1]*, Wenjing Xu[2], Huiqing Liu[1]

[1]*State Key Laboratory of Petroleum Resources and Engineering, China University of Petroleum, Beijing 102249, P. R. China*
[2]*PetroChina Dagang Oilfield Company, Tianjin 300280, P. R. China*

Keywords:
Heavy oil reservoirs
cyclic multi-thermal fluid stimulation
mathematical model
horizontal well
production performance

Cited as:
Jiang, X., Dong, X., Xu, W., H, Liu. A productivity model for multi-thermal fluid huff-n-puff in horizontal wells: Application to heavy oil reservoirs. Computational Energy Science, 2025, 2(2): 68-84.
https://doi.org/10.46690/compes.2025.02.04

Abstract:
Cyclic steam stimulation using vertical wells has been widely employed in the exploitation of heavy oil reservoirs. However, during the later stages, this method encounters significant challenges, including high water cut and substantial heat loss. In contrast, the application of cyclic multi-thermal fluid stimulation in horizontal wells offers a more effective and sustainable alternative. Accordingly, this paper presents a production performance prediction model for cyclic multi-thermal fluid stimulation in horizontal wells. Firstly, based on the contact relationship between heated zone and reservoir boundaries, an improved heating radius evolution model is established by considering the nonlinear temperature distribution behavior in hot-water zone. Then, a staged productivity model is derived by applying the equivalent flow resistance method. Following this, the solution methodology for the productivity model is described, and subsequently the proposed model is also validated by comparing against the field data from a typical heavy oil reservoir subjected to cyclic multicomponent thermal fluid stimulation via horizontal wells. Finally, a sensitivity analysis is conducted to investigate the impacts of key reservoir properties and operational parameters. The calculated daily oil production rate and cumulative oil production from our model show a trend consistent with field data, with a cumulative production error of 4.0%, confirming the model's applicability for subsequent analysis. Compared with conventional heavy oil, the extra-heavy and ultra-heavy crude oils can demonstrate a notable reduction in both cumulative oil production and cumulative oil-steam ratio. Bottom-hole pressure reduction and non-condensable gas injection can effectively improve both the cumulative oil-steam ratio and oil production. Additionally, increasing the cyclic injection volume exhibits a diminishing marginal effect on enhancing oil production. Our study offers an effective forecast approach for the production performance of cyclic multi-thermal fluid stimulation in horizontal wells.

1. Introduction

Heavy oil resources constitute a vital component in securing hydrocarbon supply. According to statistics from the American Association of Petroleum Geologists (AAPG), the worldwide resources of bitumen and heavy oil amount to 938 billion tons, with over 80% located in Canada, Venezuela, and the United States (Dong et al., 2019; Pratama and Babadagli, 2022; Sun et al., 2022). Heavy oil serves not only as a significant energy source but also as a vital feedstock for the chemical industry (e.g., high-end lubricants, specialty transformer oils), thereby providing a solid foundation for global sustainable development (Guan et al., 2022). However, due to the high content of heavy components such as resins and asphaltenes, heavy oil exhibits poor mobility under reservoir conditions (Pratama and Babadagli, 2022; Thangarajn and Lee, 2024; Aliev et al., 2025). Enhancing the mobility of heavy oil thus becomes a critical focus. Based on the mechanism of reducing oil viscosity, heavy oil recovery techniques are broadly grouped into cold production (Kantzas and Brook, 2004; Jia et al., 2013; Zhu et al., 2022; Ogunkunle et al., 2025), thermal methods (Kirmani et al., 2021; Dong et al., 2024; Zhao et al., 2024; Jiang et al., 2025; Yan

Yandy Scientific Press

*Corresponding author.
E-mail address: jiangxc9808@163.com (X. Jiang); dongxh@cup.edu.cn (X. Dong,); xuwenjingll@163.com (W. Xu); liuhq@cup.edu.cn (H. Liu).

Received April 23, 2025; revised May 9, 2025; accepted June 18, 2025; available online June 23, 2025.

et al., 2025), and hybrid thermal approaches (Bruns and Babadagli, 2020; Dong et al., 2022; Pérez et al., 2022; Lu et al., 2024; Lin et al., 2025). Among these methods, steam injection is the most prevalent thermal recovery process for heavy oil reservoirs, notably in applications such as cyclic steam stimulation (CSS), steam flooding (SF), and steam-assisted gravity drainage (SAGD) (Luo et al., 2020; Sun et al., 2023; Pratama and Babadagli, 2024). To enable more efficient development of heavy oil reservoirs, the adoption of advanced well configurations and enhanced injection fluids is standard practice. Therefore, the combination of horizontal wells with multicomponent thermal fluids represents one of the pivotal techniques for achieving high-efficiency recovery (Hou et al., 2016; Dong et al., 2020).

The depletion of conventional hydrocarbon resources, coupled with continuous advancements in drilling, has established horizontal wells as a technology critical for unlocking unconventional resources such as low-permeability, thin-bed, and heavy-oil reservoirs (Biglarbigi et al., 2000; Li et al., 2018; Hu et al., 2023). The primary advantages of horizontal well development include increased reservoir contact area and well productivity, reduced production pressure differential and operational costs, enhanced hydrocarbon recovery, and a decreased number of required wells and surface footprint (Catania, 2000; Hou et al., 2016; Pang et al., 2020). For heavy oil reservoirs specifically, horizontal wells can dramatically improve steam injectivity and enlarge the thermal sweep volume (Escobar et al., 2000; Hou et al., 2016; Dong et al., 2020). Given that cold production typically yields only a 10%-15% recovery factor in Western Canada's thin heavy-oil reservoirs, Zhao et al. (2014) employed reservoir simulation to compare several thermal recovery processes, including SAGD, steam flooding, and hot water flooding, where all development scenarios utilized horizontal wells. The results indicated that both SAGD and steam flooding achieved favorable recovery factors approaching 40%. However, this enhanced recovery exhibited high energy intensity, with the cumulative energy injected per unit volume of oil produced reaching 32.9 GJ/m^3 for SAGD and 13.6-20.9 GJ/m^3 for steam flooding under varying well spacing configurations. Huang et al. (2019) investigated solvent-enhanced steam flooding (SESF) using horizontal wells through two-dimensional physical simulations to overcome the limitations of steam flooding in thin heavy-oil reservoirs, such as low thermal efficiency and limited sweep. Their results demonstrated that SESF, across a range of solvent-to-steam ratios, achieved a substantial expansion of the steam chamber and improved the oil recovery factor from 21% to 34%-58%. For thick heavy oil reservoirs, Wang et al. (2024) conducted laboratory-scale physical simulations to investigate the evolution of the heated zone during cyclic steam stimulation with horizontal wells (CSSHW). It was observed that the temperature within the heated zone progressively decreased with increasing distance from the wellbore within the same cycle. Additionally, at a given location, the temperature increased with successive cycles due to the effects of residual heat. Yan et al. (2025) carried out a comparative study employing 3D physical experiments on two horizontal well steam flooding schemes: conventional (CSF) and tridimensional (TSF). They found that TSF yielded a higher oil recovery (53% vs. 43% for CSF) and achieved an approximately threefold expansion of the steam chamber. The conventional development method for extra-heavy oil reservoirs is SAGD. The core mechanism involves using a horizontal well pair to homogeneously reduce the oil viscosity across the reservoir, thereby establishing the conditions for efficient gravity drainage. (Soler et al., 2023; Dong et al., 2024; Li et al., 2025). Another significant application involves using horizontal wells to develop heavy oil reservoirs with underlying aquifers (Pang et al., 2020; Hu et al., 2023; Zhou et al., 2025).

On the other hand, it has been established in the literature that the non-condensable gases (NCG) in multicomponent thermal fluids play key enhancement roles in exploiting heavy oil reservoirs, primarily by improving heat retention, providing pressure maintenance, and reducing oil viscosity (Dong et al., 2015; Hou et al., 2016; Huang et al., 2018; Jiang et al., 2024; Chen et al., 2025). Studies on heavy oil recovery via multicomponent thermal fluids typically encompass wellbore flow and heat transfer (Dong et al., 2016; Sun et al., 2018; Nie, 2022; Wang, 2023), reservoir performance enhancement (Jamshid-nezhad, 2022; Wang et al., 2023; Li et al., 2025; Weng et al., 2025), and field application (Liu et al., 2011; Tang et al., 2011; Austin-Adigio and Gates, 2019; Yi et al., 2021; Lin et al., 2025). Dong et al. (2016) employed a wellbore discretization and nodal analysis approach to investigate flow behavior and model the process in horizontal heavy oil wells under gas-steam co-injection. Their study demonstrated that this co-injection method extends the effective thermal length and improves heating efficiency compared to conventional steam injection. For the multi-point steam injection process in horizontal wells, Sun et al. (2018) developed a heat and mass transfer model for multicomponent thermal fluids within the wellbore to investigate their behavior, examining the impact of varying fluid compositions on the annulus mass flow rate of non-condensable gases and the formation heat absorption rate. Nie (2022) and Wang (2023) respectively established models for the wellbore preheating process during multicomponent thermal fluid circulation, based on their considerations of the flow and heat transfer characteristics of superheated steam and non-condensable gases. Numerical simulations by Jamshid-nezhad revealed that steam alternating non-condensable gas (SANG) injection outperforms SAGD and SAGP in steam chamber expansion, owing to the insulating barrier formed by NCG, which enhances the efficacy of subsequent steam re-injection (Jamshid-nezhad, 2022). Experimental investigation by Wang et al. (2023) on the hybrid steam-gas huff-n-puff process with varying NCG compositions demonstrated a non-monotonic relationship between CO_2 concentration and oil recovery. The recovery factor initially increases but then declines with higher CO_2 content, yielding an optimal N_2/CO_2 ratio of 2:1, which corresponds to a maximum recovery of 31%. Weng et al. (2025) experimentally evaluated various flue gas injection strategies for heavy oil recovery. They demonstrated that a slug injection scheme achieves optimal performance when the flue gas is introduced during a relatively mature phase of steam chamber development. Li et al. (2025) conducted experiments to investigate the gas-assisted vertical-horizontal well hybrid

SAGD (VH-SAGD) process. They found that flue gas injection better utilizes the advantages of the well architecture, thereby increasing the ultimate oil recovery from 58.9% to 71.7% compared to the conventional VH-SAGD method. Field data from the Bohai Oilfield in China confirm that cyclic multi-thermal fluid stimulation boosted the peak oil production rate by a factor of 2.5 to 5.4 over cold production (Liu et al., 2011; Tang et al., 2011; Lin et al., 2025). MEG Energy's SAGP pilot test demonstrated that the enhanced modified steam assisted gas push (eMSAGP) process reduced the steam-to-oil ratio to below 2 m^3/m^3. Temperature profiles from observation wells concurrently indicated that non-condensable gas (NCG) injection promoted vertical expansion of the steam chamber (Austin-Adigio and Gates, 2019). Successful field applications in Kazakhstan have positioned cyclic multi-thermal fluid huff-n-puff as the key successor to conventional steam stimulation for shallow heavy oil reservoirs (Yi et al., 2021).

Conventional productivity analysis fails for thermal huff-n-puff due to its non-isothermal flow, which requires modeling temperature-dependent viscosity and relative permeability (Hou et al., 2016; Jiang et al., 2024; Wang et al., 2024). This challenge is often addressed by modeling the reservoir as a composite of heated and cold regions using hydrodynamic analogy. The determination of the heated radius is a critical step in productivity evaluation. The original formula for this calculation was proposed by Marx and Langenheim (1959), establishing a fundamental basis for the subsequent development of huff-n-puff productivity models (Boberg and Lantz, 1966; Jones, 1977; Gros et al., 1985). A common thread among the productivity models proposed by Boberg and Lantz (1966), Jones (1977), and Gros et al. (1985) is the adoption of an assumption that a uniform temperature prevails in the heated zone at the end of injection, implying a distinct thermal discontinuity at its interface with the cold region. Li and Yang (2003) derived formulas for both the heated radius and initial production rate by incorporating a linearly decreasing temperature profile in the heated zone into their model. Building on a heated-zone structure of steam and hot-water regions, He et al. (2015) proposed an improved productivity model that incorporates a thermal front temperature via the viscosity-temperature relationship. The model outputs were compared against those from the Boberg-Lantz isothermal model and numerical reservoir simulation. Wu et al. (2018) introduced new models for heated radius and productivity in N_2-assisted cyclic steam stimulation by incorporating an exponential temperature profile for the hot-water zone, with solutions achieved via iterative methods. Dong et al. (2025) developed a productivity model for cyclic supercritical multi-thermal fluid stimulation by incorporating experimental data on temperature-dependent relative permeability. The models discussed above employ different temperature distributions within the heated zone. In reality, the temperature profile directly impacts the accurate calculation of the heated radius. Furthermore, numerous studies have indicated that the temperature in the hot-water zone exhibits a nonlinear distribution (Cheng et al., 2019; Sun et al., 2023; Jiang et al., 2024; Wang et al., 2024). Based on the contact dynamics between the heated zone and reservoir boundaries and the equivalent seepage resistance method, Zhang et al. (2021) developed stage-wise models for heated radius and productivity in horizontal well cyclic steam stimulation. The model for horizontal well multi-thermal fluid huff-n-puff productivity, developed by Hou et al. (2016), incorporates CO_2-dissolution-induced viscosity reduction. It utilizes the correlation proposed by Chung et al. (1988) for CO_2 solubility in heavy oil and employs an Arrhenius-type model to characterize the viscosity of the resulting oil-CO_2 mixture. Besides, an alternative approach approximates the productivity of a horizontal well by summing the contributions from discrete vertical wellbore segments. Wu et al. (2011) accounted for the effects of gravity and developed a productivity model for cyclic steam stimulation in horizontal wells within heavy oil reservoirs. From the above discussion, four distinct huff-n-puff productivity models are identified, depending on the well type and injection fluid: vertical well with steam, vertical well with multi-component thermal fluid, horizontal well with steam, and horizontal well with multi-component thermal fluid. In the model of Hou et al. (2016), the reservoir is represented as a composite system consisting of a heated zone and a cold zone, with the assumption of a uniform temperature distribution in the heated zone upon termination of steam injection. Thus, to better align with actual reservoir properties, a multi-component thermal fluid huff-n-puff productivity model is developed in this study for a composite reservoir system. The system consists of steam, hot-water, and cold zones, accounting for the nonlinear temperature distribution featured in the hot-water zone.

In this paper, a prediction model of production performance for cyclic multicomponent thermal fluid stimulation in horizontal wells is established. In Section 2, based on the contact relationship between the heated zone and the reservoir boundaries, characterization models for the heating radius evolution are first established, incorporating the nonlinear temperature distribution in the hot-water zone. Subsequently, staged productivity models are developed using the equivalent seepage resistance method. Finally, the corresponding auxiliary equations for computing key parameters (e.g., temperature, pressure, and water saturation) are formulated to enable the solution of the productivity equation. In Section 3, the primary solution procedure for the productivity model is presented. The model is then validated against field production data from a typical heavy oil reservoir developed by horizontal well, cyclic multicomponent thermal fluid stimulation. Furthermore, a sensitivity analysis is conducted to investigate the impacts of key reservoir properties and operational parameters. In Section 4, the main conclusions of this study are summarized.

2. Model description

Following the injection of multi-thermal fluid (a mixture of steam, nitrogen, and carbon dioxide), as shown in Fig. 1, a composite reservoir model is formed, consisting of three distinct non-isothermal zones: A steam area (SA), a hot-water area (HA), and a cold area (CA). The steam zone remains at the injected steam temperature, while the cold zone remains at the original reservoir temperature. The temperature in the hot-water zone decreases exponentially from the steam

temperature to the original reservoir temperature. Based on the equivalent flow resistance principle, the complex flow behavior around the horizontal well is simplified into two regions, as illustrated in Fig. 2, a horizontal radial flow in the far-well region and a vertical radial flow in the near-wellbore region. When establishing a productivity mathematical model to describe the huff-n-puff development process, the following fundamental assumptions are considered:

1) The flow behavior is characterized by a total resistance that equals the combined resistance from both horizontal and vertical flow.
2) A homogeneous and isotropic reservoir is assumed, and the effect of steam/gas overlay is neglected.
3) Throughout the same stimulation cycle, the heated radius is held constant following the injection period, with the temperature in the heated zone declining gradually during the production period due to heat conduction and convective loss from fluid production.
4) A constant injection rate and an even distribution of the multi-thermal fluid are maintained along the horizontal well section.
5) The mechanisms associated with non-condensable gases during the huff-n-puff process are considered, including heat transport by non-condensable gases, viscosity reduction due to carbon dioxide dissolution, and energy enhancement from nitrogen.
6) Within the cold zone, heavy oil is modeled as a non-Newtonian fluid, which possesses a threshold pressure gradient.

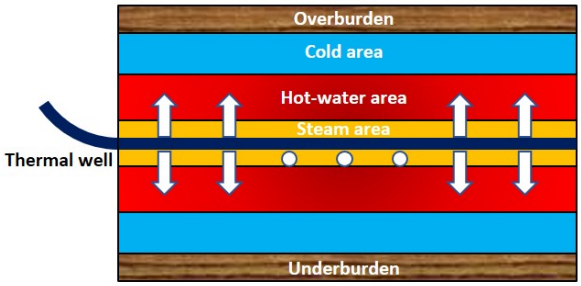

Fig. 1. Schematic of a horizontal well with multi-thermal fluid huff-n-puff process in a heavy oil reservoir.

2.1 Heated radius model

Based on the contact conditions between the steam/hot-water zones and the top/bottom boundaries of the reservoir, the expansion behavior of the heated zone involves three distinct stages, characterized sequentially by: absence of contact between the hot-water zone and the boundaries, contact of only the hot-water zone, and finally contact of the steam zone.

During the first stage, neither the steam zone nor the hot-water zone is in contact with the top and bottom boundaries of the reservoir, as illustrated in Fig. 2. Therefore, heat loss to the overburden and underburden is neglected. As governed by the law of energy conservation, the heat input rate to the reservoir equals the energy accumulation rate in the formation, which, within the steam zone, is manifested as the latent heat from the injected steam (Zhang et al., 2021):

$$q_s \cdot x \cdot L_v = M_R \cdot \frac{dA_s}{dt} \cdot L \cdot (T_s - T_i) \tag{1}$$

The radius of SA can be determined from Eq. (1).

$$r_s = \sqrt{\frac{q_s \cdot x \cdot L_v \cdot t}{M_R \cdot L \cdot \pi (T_s - T_i)} + r_w^2} \tag{2}$$

where q_s is the steam injection rate, kg/d; x is the steam quality; L_v is the latent heat of vaporization of steam, kJ/kg; M_R is the volumetric heat capacity of the reservoir, kJ/(m^3·°C); A_s is the area of SA, m^2; t is the steam injection duration, d; L is the horizontal section length, m; T_s is the injection temperature, °C; T_i is the original formation temperature, °C; r_w is the wellbore radius, m; r_s is the radius in SA, m.

Similarly, the energy conservation relationship for the hot-water zone can be established, where the injected heat comprises the enthalpy of saturated hot-water and the enthalpy of non-condensable gas components:

$$H_m = M_R \cdot \frac{dA_h}{dt} \cdot L \cdot (T_h - T_i) \tag{3}$$

where

$$H_m = q_s \cdot (h_{ws} - h_{wr}) + q_n \cdot (h_{ns} - h_{nr}) + q_c \cdot (h_{cs} - h_{cr}) \tag{4}$$

To better approximate actual reservoir conditions, a dimensionless temperature distribution relationship is employed to characterize the temperature profile in the hot-water zone at the end of the injection period (Jiang et al., 2024):

$$T_h = T_i + (T_s - T_i)\, e^{-3.665 \frac{r - r_s}{r_h - r_s}} \tag{5}$$

where H_m is the heat injection rate into the hot-water zone, kJ/d; A_h is the area of HA, m^2; T_h is the temperature of HA at the end of the injection period, °C; h_{ws}, h_{ns}, and h_{cs} are the enthalpies of water, nitrogen, and carbon dioxide, respectively, at saturated water temperature, kJ/kg; h_{wr}, h_{nr}, and h_{cr} are the enthalpies of water, nitrogen, and carbon dioxide, respectively, at original formation temperature, kJ/kg; q_n and q_c are the injection rates of nitrogen and carbon dioxide, respectively, kg/d; r_h is the radius in HA, m.

For the second stage, the radius of steam zone can be obtained by Eq. (1). For hot-water zone, the energy conservation relationship can be expressed as Eq. (6):

$$H_m = M_R \cdot \frac{dA_h}{dt} \cdot h \cdot (T_h - T_i) + 2 \int_0^t \frac{\lambda_e (T_h - T_i)}{\sqrt{\pi \alpha_e (t - t_2)}} dA_h \tag{6}$$

where λ_e is the heat conductivity of overburden and underburden, kJ/(d·m·°C); α_e is the heat diffusivity of overburden and underburden, m^2/d; t_2 is the time at which the hot-water zone begins to contact the top and bottom boundaries of the reservoir, d.

Regarding the third stage, the energy conservation of hot-water zone satisfies Eq. (6). For steam zone, the energy conservation relationship can be expressed as Eq. (7):

$$q_s \cdot x \cdot L_v = M_R \cdot \frac{dA_s}{dt} \cdot h \cdot (T_s - T_i) + 2 \int_0^t \frac{\lambda_e (T_s - T_i)}{\sqrt{\pi \alpha_e (t - t_3)}} dA_s \tag{7}$$

where t_3 is the time at which the steam zone begins to contact

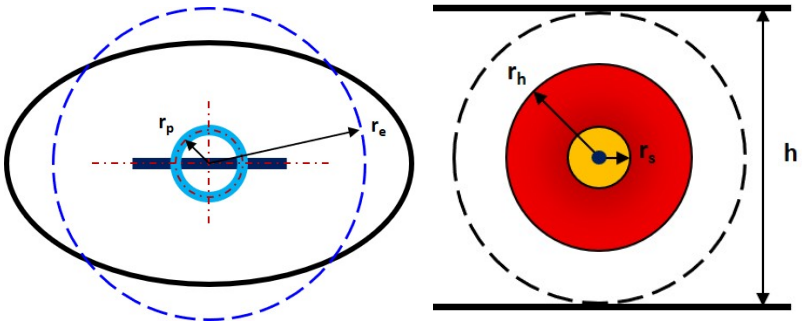

(a) Horizontal radial flow (b) Vertical radial flow

Fig. 2. Equivalent flow behavior around the horizontal well.

the top and bottom boundaries of the reservoir, d.

Substituting Eq. (5) into Eqs. (3) and (6), the heated radius of hot-water zone could be iteratively solved, respectively.

2.2 Productivity model

From the equivalent division of flow behavior around the horizontal well in Fig. 2, horizontal flow occurs entirely within the cold zone, whereas vertical planar flow encompasses three distinct regions: the steam zone, the hot-water zone, and the cold zone. Based on the model assumptions and considering the threshold pressure gradient in the cold zone, the equivalent flow resistance method is applied to determine the crude oil production (under surface conditions) for cyclic multi-thermal fluid stimulation in heavy oil reservoirs using horizontal wells:

$$Q_o = \frac{0.0864\left(P_{avg} - P_{wf} - G\cdot(r_e - r_h)\right)}{R_{o,in} + R_{o,out}} \tag{8}$$

where Q_o is the oil productivity, m^3/d; P_{avg} is the average reservoir pressure, MPa; P_{wf} is the bottom-hole pressure, MPa; G is the threshold pressure gradient, MPa/m; r_e is the drainage radius, m; $R_{o,in}$ denotes the oil phase flow resistance within the vertical plane, $(MPa\cdot d)/m^3$; $R_{o,out}$ denotes the oil phase flow resistance within the horizontal plane, $(MPa\cdot d)/m^3$ (The equations of flow resistance are shown in Appendix A).

2.3 Auxiliary equations

To solve the productivity equation shown in Eq. (8), it is necessary to characterize the evolution of several key parameters, including reservoir temperature, pressure, and water saturation. On this basis, the crude oil viscosity and oil/water relative permeability are further determined (The detailed equations are shown in Appendix B).

3. Results and discussions

3.1 Solution methodology

The primary solution procedure for the productivity model of cyclic multi-thermal fluid stimulation in heavy oil reservoirs using horizontal wells is as follows: As described in auxiliary equations of Appendix B, key reservoir parameters (e.g., pressure, temperature, water saturation) are first determined. These parameters are then incorporated into the productivity model to obtain production performance data, such as oil production rate and cumulative oil production. A flowchart of the model solution procedure is presented in Fig. 3, and the specific steps are detailed below.

1) Input base data, including reservoir parameters, thermal properties, and injection parameters.
2) The radius of the steam zone is calculated using Eqs. (1) and (7), while the radius of the hot-water zone is obtained from Eqs. (3) and (6).
3) At the end of the soaking period, calculate the average temperatures of the steam and hot-water zones, average formation pressure, and water saturation by solving Eqs. (B2), (B3), (B6), and (B8). The daily oil production rate can be obtained from Eq. (8).
4) During the production stage, compute the average temperatures of the steam and hot-water zones, average formation pressure, and water saturation by solving Eqs. (B4), (B5), (B7), and (B8). The daily oil production rate can be determined using Eq. (8).
5) Calculate the residual heat in the heated zone using Eqs. (B14) and (B15).
6) Repeat steps (2) through (5) to obtain the production performance of multi-cycle CMTFS in heavy oil reservoir developed by horizontal wells.

3.2 Model validation

Based on the established productivity model for horizontal well cyclic multi-thermal fluid stimulation, validation is performed using production data from a typical CMTFS well of an oilfield in China. Specifically, reservoir parameters, fluid properties, and steam/gas injection parameters are input into the model during the validation process. The detailed values of these parameters are shown in Table 1. Besides, Fig. B1 illustrates the variation of oil/water relative permeability with water saturation at different temperatures. Fig. B2 presents the crude oil viscosity at different temperatures.

To more accurately represent actual reservoir performance, dynamic changes in field-measured bottom-hole flowing pressure were incorporated into the model, as illustrated in Fig. 4. Then, the oil production is calculated, and the comparisons between model results and field production performance are

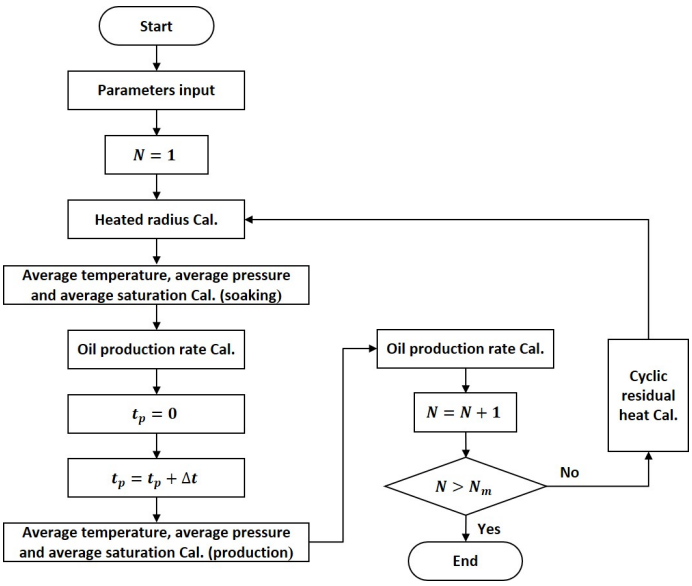

Fig. 3. Flowchart of the productivity model solution.

Table 1. Main parameters used for model validation.

Type	Parameter	Value
Reservoir property	Reservoir thickness	8 m
	Porosity	0.35
	Permeability	3045×10^{-3} μm^2
	Original reservoir pressure	8.8 MPa
	Original reservoir temperature	56 °C
	Original water saturation	0.26
	Reservoir compressibility	0.01 MPa^{-1}
Fluid property	Specific heat capacity of oil	2.1 kJ·kg^{-1}·°C^{-1}
	Specific heat capacity of water	4.2 kJ·kg^{-1}·°C^{-1}
	Oil formation volume factor	1.05 m^3/m^3
	Water formation volume factor	1.01 m^3/m^3
Operation parameter	Wellbore radius	0.1 m
	Horizontal section length	168 m
	Injection duration	22 d
	Soaking duration	5 d
	Production duration	445 d
	Steam injection rate (cold water equivalent)	195.5 m^3·d^{-1}
	Injection temperature	300 °C
	Steam quality	0.4
	NCG injection rate at surface conditions	51561 m^3·d^{-1}
	NCG volume composition (N_2:CO_2)	4:1

shown in Fig. 5. It can be seen that both the modeled and field-measured daily oil production rates exhibit similar overall trends. The model predicts a peak production rate of 60 m^3/d, which is in close agreement with the field-observed peak of 61 m^3/d. For cumulative oil production, the model yields a result of 20,865 m^3, while field data indicate 20,071 m^3, corresponding to a relative error of 4.0%. These results confirm the reliability of the productivity model in this paper for predicting performance in similar reservoir conditions.

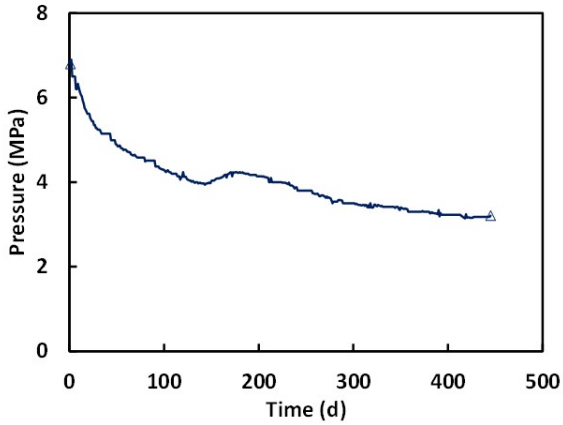

Fig. 4. The bottom-hole flowing pressure of a typical CMTFS well.

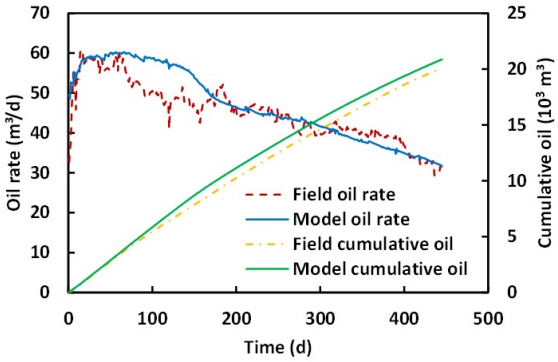

Fig. 5. Comparison of modeled and field oil production.

3.3 Sensitivity analysis

The validated productivity model is employed to conduct a sensitivity analysis. The selected parameters include permeability, initial water saturation, crude oil type, cyclic injection volume, bottom-hole flowing pressure, and injection fluid type. The first three parameters are reservoir properties, while the latter three are operational parameters. The values of each parameter are presented in Table 2, and the viscosity-temperature curves for conventional heavy oil, extra-heavy oil, and super-heavy oil are shown in Fig. 6.

In the base case for calculating multi-cycle huff-n-puff productivity, the fundamental parameters are as follows: the original reservoir temperature is 50 °C; the reservoir permeability is $3,000 \times 10^{-3}$ μm^2; the original water saturation is 0.25; the reservoir thickness is 32 m; the crude oil type is the conventional heavy oil shown in Fig. 6; the number of huff-n-puff cycles is three; the durations for the injection, soaking, and production phases in each cycle are 22, 5, and 338 days, respectively; the cyclic steam injection volume is 4,400 m^3; the bottom-hole pressures for the three cycles are 6.0, 5.0, and 4.0 MPa, respectively; the injected fluid is mixture of flue gas and steam; and the values of all other parameters are consistent with those provided in Table 1. The relative permeability curves employed in the base case are shown in Fig. B1.

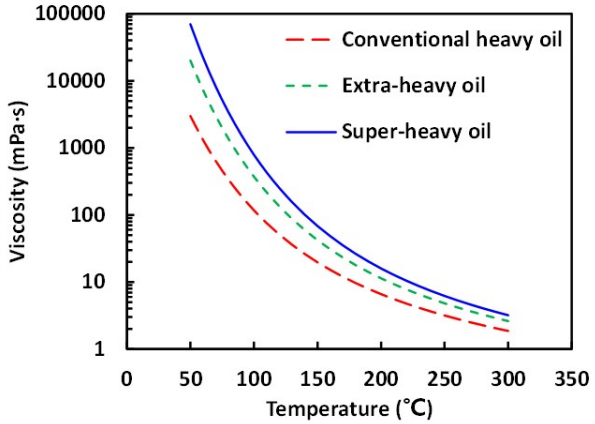

Fig. 6. Viscosity-temperature curves for different crude oil types.

By inputting the aforementioned data into the established productivity model, the production performance of the base case can be obtained. Fig. 7(a) shows the oil rate and cumulative oil for the base case. Firstly, it can be found that the maximum oil rate gradually decreases with increasing huff-n-puff cycles, with the daily peak rates for the respective cycles being 69, 75, and 78 m^3/d. Secondly, it can be found that the third cycle yields the highest cumulative oil production (18,009 m^3), accounting for 35% of the total oil production from the three cycles. This result is attributed to the progressive decline in bottom-hole pressure, which amplifies the production drawdown. Fig. 7(b) shows the cumulative oil-steam ratio variation over time for the base case. The maximum cumulative oil-steam ratio also exhibits a gradual increase over successive cycles, with values of 3.52, 3.72, and 3.84 m^3/m^3 at the end of each cycle, respectively.

3.3.1 Reservoir properties

Firstly, the effects of reservoir permeability on cumulative oil production and the oil-steam ratio are compared in Fig. 8. It is observed that both cumulative oil production and the cumulative oil-steam ratio exhibit a gradual increase with increasing reservoir permeability. As can be seen from Fig. 8(a), an increase in reservoir permeability from 1,000 to $2,000 \times 10^{-3}$ μm^2 results in an incremental cumulative oil production of 16,579 m^3. In contrast, increasing the permeability from 4,000 to $5,000 \times 10^{-3}$ μm^2 yields a much smaller increment of only 6,191 m^3. In addition, the comparative results in Fig. 8(b) show that the cumulative oil-steam ratio rises from 1.71 to 2.97 m^3/m^3 when permeability increases from 1,000

Table 2. Values of different influencing factors.

Parameter	Value				
Permeability (10^{-3} μm^2)	1,000	2,000	3,000	4,000	5,000
Original water saturation	0.25	0.30	0.35	0.40	0.45
Cyclic steam injection volume (m^3)	2,200	3,300	4,400	5,500	6,600
Bottom-hole pressure (MPa)	7.0	6.5	6.0	5.5	5.0
	6.0	5.5	5.0	4.5	4.0
	5.0	4.5	4.0	3.5	3.0
Injected fluid	Steam	N_2-steam	CO_2-steam	Flue-steam	
Crude oil type	Conventional heavy oil	Extra-heavy oil	Super-heavy oil		

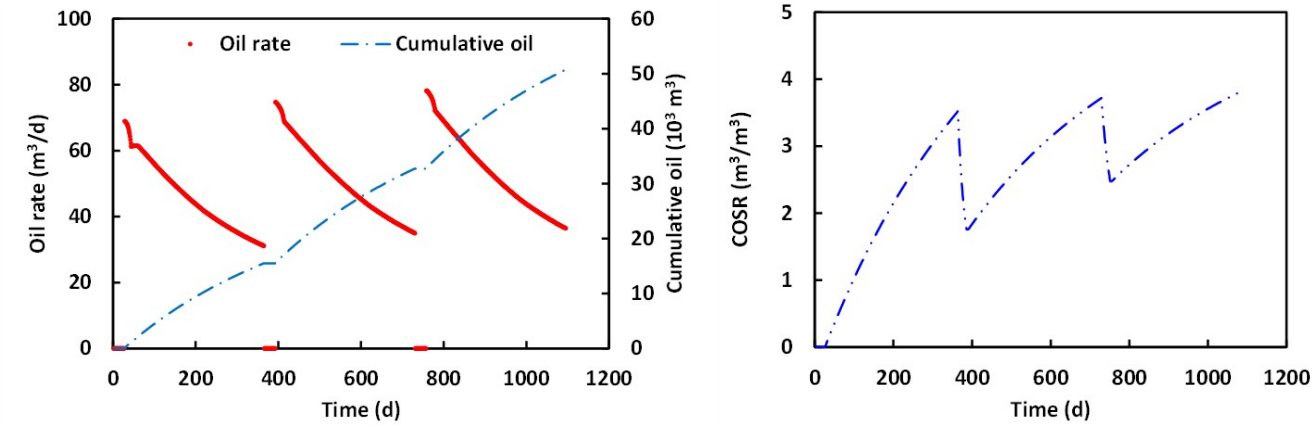

(a) Oil rate and cumulative oil (b) Cumulative oil-steam ratio (COSR)

Fig. 7. Production performance of the base case.

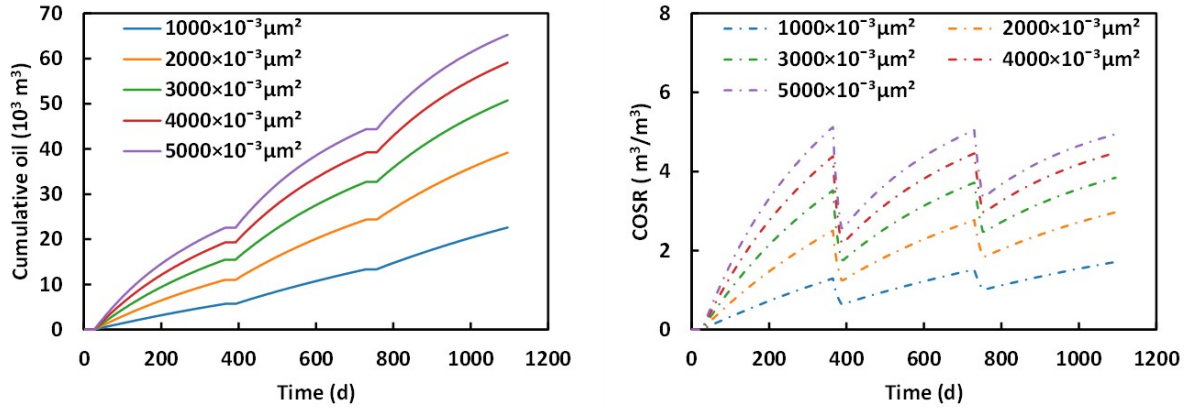

(a) Cumulative oil (b) Cumulative oil-steam ratio (COSR)

Fig. 8. Effects of permeability on production performance.

to $2,000 \times 10^{-3}$ μm^2, whereas it only increases from 4.48 to 4.95 m^3/m^3 for the permeability increase from 4,000 to $5,000 \times 10^{-3}$ μm^2. These results indicate that enhancing reservoir permeability leads to a more substantial production improvement in lower-permeability formations. For oil production and the cumulative oil-steam ratio across different cycles, at a reservoir permeability of $1,000 \times 10^{-3}$ μm^2, the cumulative oil production and oil-steam ratio for the three cycles are 5,699, 7,674, and 9,233 m^3 and 1.30, 1.52, and 1.71 m^3/m^3, respectively. When the permeability is increased to $4,000 \times 10^{-3}$ μm^2, the corresponding values are 19,290, 19,947, and 19,849 m^3 and 4.38, 4.46, and 4.48 m^3/m^3. These results indicate that reducing the bottom-hole pressure is more effective in lower-permeability reservoirs.

Next, the effects of original water saturation on cumulative oil production and the oil-steam ratio are compared in Fig. 9(a). It is observed that as the original water saturation increases, both cumulative oil production and the cumulative oil-steam ratio gradually decline. As shown in Fig. 9, an increase in initial water saturation from 0.25 to 0.30 results in a reduction in cumulative oil production of only 3,355 m^3. However, a further increase from 0.30 to 0.35 leads to a more substantial decrease of 10,376 m^3. Moreover, the comparative results in Fig. 9(b) indicate that the cumulative oil-steam ratio declines from 3.84 to 3.59 m^3/m^3 as the initial water saturation rises from 0.25 to 0.30. A subsequent increase in saturation from 0.30 to 0.35 causes the ratio to drop further from 3.59 to 2.80 m^3/m^3. These results can be explained by the influence of water saturation on oil relative permeability. Considering the temperature dependence of relative permeability endpoints (Fig. B1), the initial water saturation of 0.25 is lower than the irreducible water saturation; therefore, any increase in water saturation within this range has a relatively minor effect on oil relative permeability, while the increase in initial water saturation from 0.30 to 0.35 corresponds to the most pronounced reduction in oil relative permeability. Subsequently, as water saturation continues to rise, the magnitude of reduction in oil relative permeability diminishes.

Furthermore, the effects of crude oil type on cumulative oil production and the oil-steam ratio are compared in Fig. 10. It is observed that significant differences exist in productivity among different crude oil types. From Fig. 10(a), when the crude oil changes from super-heavy oil to extra-heavy oil, the cumulative oil production increases from 7,757 to 23,705 m^3. A further change to conventional heavy oil results in a corresponding increase to 50,738 m^3. Additionally, comparative results in Fig. 10(b) show that the cumulative oil-steam ratios for super-heavy oil, extra-heavy oil, and conventional heavy oil are 0.59, 1.80, and 3.84 m^3/m^3, respectively. The viscosity-temperature curves for the different crude oil types simulated in this section are presented in Fig. 6, with viscosities at 50 °C being 3,000, 2,0000, and 70,000 mPa·s for conventional heavy oil, extra-heavy oil, and super-heavy oil, respectively. According to Eq. (8), oil production rate of huff-n-puff process is negatively correlated with crude oil viscosity. Consequently, both oil production and the oil-steam ratio decrease significantly as crude oil viscosity increases.

3.3.2 Operation parameters

Firstly, the effects of cyclic steam injection volume on cumulative oil production and the oil-steam ratio are compared in Fig. 11. With increasing cyclic injection volume, cumulative oil production gradually increases, while the cumulative oil-steam ratio gradually decreases. As shown in Fig. 11(a), an increase in the cyclic injection volume from 2,200 to 3,300 m^3 results in an incremental cumulative oil production of 3,979 m^3, whereas an increase from 5,500 to 6,600 m^3 yields a smaller increment of only 2,313 m^3. Besides, comparative results in Fig. 11(b) indicate that the cumulative oil-steam ratio declines from 6.55 to 4.77 m^3/m^3 when the injection volume increases from 2,200 to 3,300 m^3, and from 3.25 to 2.82 m^3/m^3 for the increase from 5,500 to 6,600 m^3. These results demonstrate that increasing the cyclic injection volume exhibits a diminishing marginal effect on enhancing oil production. Increasing the cyclic injection volume has a dual effect: it enhances the heat input into the reservoir while simultaneously raising the water saturation within the reservoir. Meanwhile, the cumulative oil-steam ratio progressively decreases as the cyclic injection volume rises.

Next, the effects of bottom-hole pressure on cumulative oil production and the oil-steam ratio are compared in Fig. 12. Reduction in bottom-hole pressure results in a notable increase in both cumulative oil production and the cumulative oil-steam ratio. Taking the third huff-n-puff cycle as an example, Fig. 12(a) indicates that a reduction in bottom-hole pressure from 4 to 3 MPa increases cumulative oil production by 9,208 m^3. Correspondingly, results in Fig. 12(b) show that the oil-steam ratio rises from 3.84 to 4.54 m^3/m^3. The reduction in bottom-hole pressure leads to a continuous increase in the production drawdown. As expressed in Eq. (8), a larger drawdown results in a higher oil production rate, thereby enhancing both cumulative oil production and the cumulative oil-steam ratio.

Furthermore, the effects of injected fluid on cumulative oil production and the oil-steam ratio are compared in Fig. 13. The addition of non-condensable gases significantly improves development performance compared to pure steam injection. As can be seen from Fig. 13(a), carbon dioxide, nitrogen, and flue gas assisted steam injection can enhance oil production by 11,752, 5,608, and 9,229 m^3, respectively, over the base case of pure steam injection (41,508 m^3. Furthermore, comparative results in Fig. 13(b) indicate that, relative to the cumulative oil-steam ratio of 3.14 m^3/m^3 for steam-only injection, the ratios for the three aforementioned non-condensable gas assisted processes are increased by 0.89, 0.42, and 0.70 m^3/m^3, respectively. The simulation results demonstrate that carbon dioxide provides a greater production enhancement than nitrogen, with flue gas ranking between the two.

4. Conclusions

In this paper, a new production performance prediction model for the cyclic multi-thermal fluid stimulation (CMTFS) process in horizontal wells has been developed for heavy oil reservoirs. The main conclusions drawn from this study are summarized as follows:

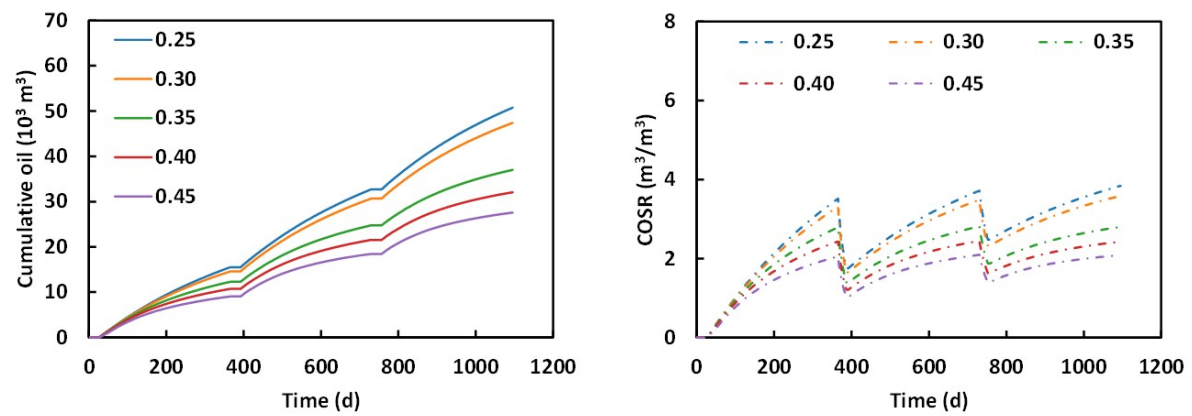

(a) Cumulative oil (b) Cumulative oil-steam ratio (COSR)

Fig. 9. Effects of original water saturation on production performance.

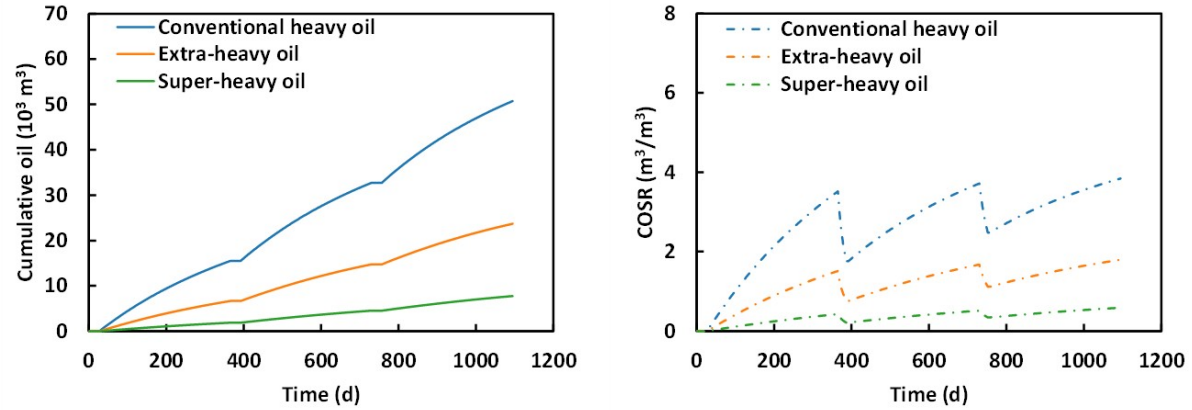

(a) Cumulative oil (b) Cumulative oil-steam ratio (COSR)

Fig. 10. Effects of crude oil type on production performance.

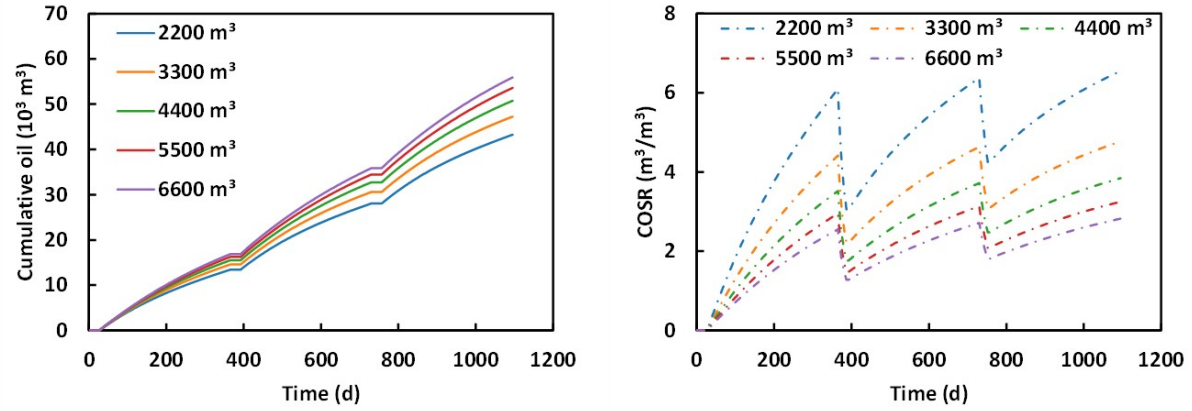

(a) Cumulative oil (b) Cumulative oil-steam ratio (COSR)

Fig. 11. Effects of cyclic steam injection volume on production performance.

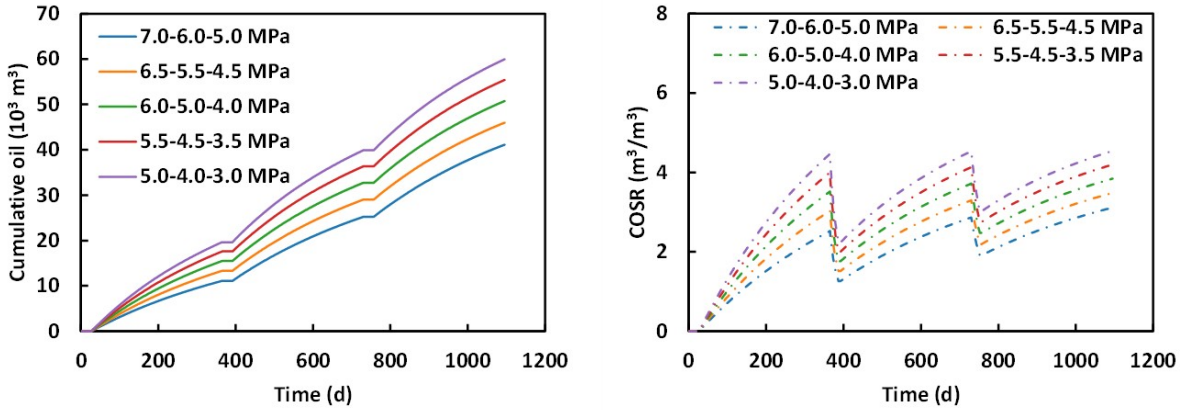

(a) Cumulative oil (b) Cumulative oil-steam ratio (COSR)

Fig. 12. Effects of bottom-hole pressure on production performance.

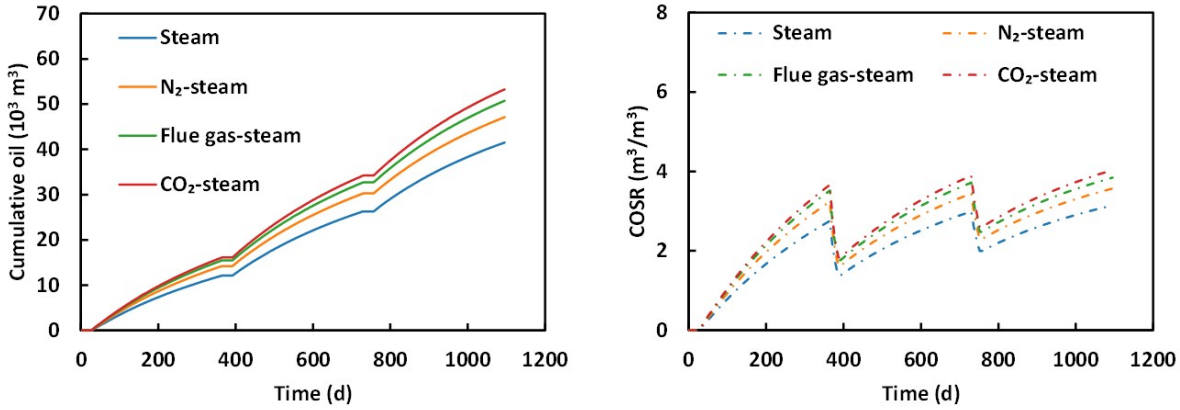

(a) Cumulative oil (b) Cumulative oil-steam ratio (COSR)

Fig. 13. Effects of injected fluid on production performance.

- Based on a hydrodynamic analogy, a productivity model is derived for the CMTFS process in horizontal wells applied to heavy oil reservoirs, which accounts for the nonlinear temperature profile in the hot-water zone and the crude oil mobility-dependent threshold pressure gradient in the cold zone.
- In addition to the mechanisms of steam stimulation, the model further incorporates the contribution of non-condensable gases, including heat transport by non-condensable gases, viscosity reduction due to carbon dioxide dissolution, and energy enhancement from nitrogen.
- Model verification shows that the predicted daily oil production trend matches field data. The predicted peak rate of 60 m^3/d aligns closely with the observed 61 m^3/d, and the cumulative oil production exhibits a low relative error of 4.0%, confirming the model's reliability.
- Cumulative oil production and the cumulative oil-steam ratio are significantly influenced by crude oil type and reservoir permeability. Additionally, lowering the bottom-hole flowing pressure and utilizing non-condensable gas as a steam additive yield remarkable improvements in both the COSR and total oil production. In contrast, raising the cyclic injection volume provides diminishing returns for cumulative production and adversely affects the COSR.

Acknowledgements

This work was financially supported by the New National Science and Technology Major Project for Oil and Gas Exploration and Development (Grant No. 2025ZD1407702) and the National Key R&D Program of China (Grant No. 2024YFF0508900).

Conflict of interest

The authors declare no competing interest.

References

Aliev, F., Mirzayev, O., Kholmurodov, T., et al. Experimental insights into catalytic conversion of carbon dioxide during in-reservoir hydrothermal upgrading of heavy oil. Fuel, 2025, 396: 135326.

Austin-Adigio, M., Gates, I. Non-condensable gas co-injection with steam for oil sands recovery. Energy, 2019, 179: 736-746.

Bruns, F., Babadagli, T. Heavy-oil recovery improvement by additives to steam injection: Identifying underlying mechanisms and chemical selection through visual experiments. Journal of Petroleum Science and Engineering, 2020, 188: 106897.

Boberg, T. C., Lantz, R. B. Calculation of the production rate of a thermally stimulated well. Journal of Petroleum Technology, 1966, 18(12): 1613-1623.

Biglarbigi, K., Mohan, H., Ray, R. M., et al. Potential for horizontal-well technology in the US. Journal of Petroleum Technology, 2000, 52(6): 68-75.

Catania, P. Predicted and actual productions of horizontal wells in heavy-oil fields. Applied energy, 2000, 65(1-4): 29-43.

Chen, Y., Zhou, K., An, Z., et al. Phased optimization of multi-thermal fluid flooding for enhanced oil recovery. Geoenergy Science and Engineering, 2025, 244: 213395.

Cheng, G., Pang, Z., Jiang, Y., et al. Thermodynamic analysis and prediction of reservoir temperature distribution for steam stimulation. Journal of Petroleum Science and Engineering, 2019, 183: 106394.

Chung, F. T. H., Jones, R. A., Nguyen, H. T. Measurements and correlations of the physical properties of CO_2-heavy crude oil mixtures. SPE reservoir engineering, 1988, 3(3): 822-828.

Dong, X., Liu, H., Chen, Z., et al. Enhanced oil recovery techniques for heavy oil and oilsands reservoirs after steam injection. Applied Energy, 2019, 239: 1190-1211.

Dong, X., Jiang, X., Zheng, W., et al. Discussion on the sweep efficiency of hybrid steam-chemical process in heavy oil reservoirs: An experimental study. Petroleum Science, 2022, 19(6): 2905-2921.

Dong, X., Liu, H., Zhai, Y., et al. Experimental investigation on the steam injection profile along horizontal wellbore. Energy Reports, 2020, 6: 264-271.

Dong, X., Liu, H., Hou, J., et al. Multi-thermal fluid assisted gravity drainage process: A new improved-oil-recovery technique for thick heavy oil reservoir. Journal of Petroleum Science and Engineering, 2015, 133: 1-11.

Dong, X., Liu, H., Hou, J., et al. Transient fluid flow and heat transfer characteristics during co-injection of steam and non-condensable gases in horizontal wells. Journal of China University of Petroleum (Edition of Natural Science), 2016, 40(2): 105-114.

Dong, M., Gao, Y., Peng, J., et al. Productivity analysis of cyclic supercritical multi-thermal fluid stimulation based on a novel relative permeability measurement method. Geoenergy Science and Engineering, 2025, 254: 214023.

Dong, X., Liu, H., Tian, Y., et al. A New method to reduce shale barrier effect on SAGD process: Experimental and numerical simulation studies using laboratory-scale model. SPE Journal, 2024, 29(4): 2044-2059.

Escobar, E., Valko, P., Lee, W. J., et al. Optimization methodology for cyclic steam injection with horizontal wells. Paper SPE 65525 Presented at the SPE/CIM International Conference on Horizontal Well Technology, Calgary, Alberta, Canada, 6-8 November, 2000.

Guan, W., Jiang, Y., Guo, E., et al. Heavy oil development strategy under the "Carbon Peaking and Carbon Neutrality" target. Acta Petrolei Sinica, 2023, 44(5): 826-840.

Gros, R. P., Pope, G. A., Lake, L. W. Steam soak predictive model. Paper SPE 14240 Presented at the SPE Annual Technical Conference and Exhibition, Las Vegas, Nevada, 22-26 September, 1985.

Hou, J., Wei, B., Du, Q., et al. Production prediction of cyclic multi-thermal fluid stimulation in a horizontal well. Journal of Petroleum Science and Engineering, 2016, 146: 949-958.

Hu, J., Zhang, G., Jiang, P., et al. A new method of water control for horizontal wells in heavy oil reservoirs. Geoenergy Science and Engineering, 2023, 222: 211391.

Huang, S., Chen, X., Liu, H., et al. Experimental and numerical study of steam-chamber evolution during solvent-enhanced steam flooding in thin heavy-oil reservoirs. Journal of Petroleum Science and Engineering, 2019, 172: 776-786.

Hu, J., Zhang, G., Jiang, P., et al. A new method of water control for horizontal wells in heavy oil reservoirs. Geoenergy Science and Engineering, 2023, 222: 211391.

Huang, S., Cao, M., Cheng, L. Experimental study on the mechanism of enhanced oil recovery by multi-thermal fluid in offshore heavy oil. International Journal of Heat and Mass Transfer, 2018, 122: 1074-1084.

He, C., Mu, L., Xu, A., et al. A new model of steam soaking heating radius and productivity prediction for heavy oil reservoirs. Acta Petrolei Sinica, 2015, 36(12): 1564. (in Chinese)

Jia, X., Zeng, F., Gu, Y. Pressure pulsing cyclic solvent injection (PP-CSI): A new way to enhance the recovery of heavy oil through solvent-based enhanced oil recovery techniques. Paper SPE 166453 Presented at the SPE Annual Technical Conference and Exhibition, New Orleans, Louisiana, USA, 30 September-2 October, 2013.

Jiang, X, Dong, X., Zhang, H., et al. Performance of steam injection process in layered heavy oil reservoirs: An experimental and numerical investigation. Petroleum Science, 2025.

Jiang, X., Dong, X., Xu, W., et al. Mathematical modeling for the production performance of cyclic multi-thermal fluid stimulation process in layered heavy oil reservoirs. Geoenergy Science and Engineering, 2024, 243: 213350.

Jamshid-nezhad, M. Steam alternating non-condensable gas injection for more heavy oil recovery. Energy, 2022, 240: 122476.

Jones, J. Cyclic steam reservoir model for viscous oil, pressure depleted gravity drainage reservoirs. Paper SPE 6544 Presented at the SPE California Regional Meeting, Bak-

ersfield, California, 13-15 April, 1977.

Kantzas, A., Brook, G. Preliminary laboratory evaluation of cold and post-cold production methods for heavy oil reservoirs part b: reservoir conditions. Journal of Canadian Petroleum Technology, 2004, 43(10): 39-48.

Kirmani, F. U. D., Raza, A., Gholami, R., et al. Analyzing the effect of steam quality and injection temperature on the performance of steam flooding. Energy Geoscience, 2021, 2(1): 83-86.

Lin, T., Song, H., Gu, Q., et al. Case study: Multi-component thermal fluid technology to enhance production on thin-bedded heavy oil reservoir in Bohai Bay of China. Energy Reports, 2025, 13: 2245-2254.

Lu, N., Dong, X., Liu, H., et al. Molecular insights into the synergistic mechanisms of hybrid CO_2-surfactant thermal systems at heavy oil-water interfaces. Energy, 2024, 286: 129476.

Luo, E., Fan, Z., Hu, Y., et al. An efficient optimization framework of cyclic steam stimulation with experimental design in extra heavy oil reservoirs. Energy, 2020, 192: 116601.

Li, P., Hao, M., Hu, J., et al. A new production decline model for horizontal wells in low-permeability reservoirs. Journal of Petroleum Science and Engineering, 2018, 171: 340-352.

Li, S., Wang, C., Wu, Y., et al. Experimental and numerical simulation studies on sweep efficiency in electrical heating-CO_2 assisted SAGD for heavy oil reservoirs with interbeds. Geoenergy Science and Engineering, 2025: 213941.

Li, B., Li, B., Sun, X., et al. Enhanced recovery in heavy oil reservoirs with interlayers using flue gas-assisted VH-SAGD: A 2D visualization study. Petroleum Science, 2025, 22(8): 3418-3433.

Li, C., Yang, B. Non-isothermal productivity predicting model of heavy crude oil exploited with huff and puff. Oil Drill. Prod. Technol, 2003, 25(5): 89-90.

Liu, X., Zhang, F., Huang, K., et al. Discussion about the thermal recovery of NB35-2 offshore heavy oilfield. Reservoir Evaluation and Development, 2011, 1(1-2): 61-63.

Marx, J. W., Langenheim, R. H. Reservoir heating by hot fluid injection. Transactions of the AIME, 1959, 216(1): 312-315.

Nie, B. Circulating preheating model of full-length horizontal wellbore in heavy oil reservoirs with multiple thermal fluid injection. Journal of Petroleum Science and Engineering, 2022, 208: 109215.

Ogunkunle, T. F., Jang, H. W., Syed, A. H., et al. Experimental investigation of hybrid enhanced oil recovery techniques for Ugnu heavy oil on Alaska North Slope. Petroleum Science, 2025, 22(2): 710-723.

Pérez, R. A., García, H. A., Gutiérrez, D., et al. Energy efficient steam-based hybrid technologies: Modeling approach of laboratory experiments. Paper SPE 209439 Presented at the SPE Improved Oil Recovery Conference, Virtual, 25-29 April, 2022.

Pratama, R. A., Babadagli, T. What did we learn from steam assisted gravity drainage (SAGD) applications in three decades, and what is next?. Geoenergy Science and Engineering, 2024, 232: 212449.

Pang, Z., Jiang, Y., Wang, B., et al. Experiments and analysis on development methods for horizontal well cyclic steam stimulation in heavy oil reservoir with edge water. Journal of Petroleum Science and Engineering, 2020, 188: 106948.

Pratama, R. A., Babadagli, T. A review of the mechanics of heavy-oil recovery by steam injection with chemical additives. Journal of Petroleum Science and Engineering, 2022, 208: 109717.

Sun, H., Liu, H., Wang, H., et al. Development technology and direction of thermal recovery of heavy oil in China. Acta Petrolei Sinica, 2022, 43(11): 1664-1674.

Sun, X., Wei, C., Zhang, Q., et al. Development of a generalized experimental methodology for investigating the role of steam quality on steamflooding performance. SPE Journal, 2023, 28(1): 401-414.

Soler, C. A. C., Malagueta, D. C., Martin, C. A. G. Feasibility of implementation of solar thermal energy in steam-assisted gravity drainage (SAGD) in extra-heavy oil field in Colombia. Geoenergy Science and Engineering, 2023, 222: 211463.

Sun, F., Yao, Y., Li, X. The heat and mass transfer characteristics of superheated steam coupled with non-condensing gases in horizontal wells with multi-point injection technique. Energy, 2018, 143: 995-1005.

Thangaraj, B., Lee, Y. K. Recent progress in catalytic aquathermolysis of heavy oils. Fuel, 2024, 372: 132089.

Tang, X., Ma, Y., Sun, Y. Research and field test of complex thermal fluid huff and puff technology for offshore viscous oil recovery. China offshore oil and gas, 2011, 23(3): 185-188.

Wang, B., Huang, S., Zhao, F., et al. Investigating the heated zone evolution and production performance of cyclic steam stimulation with horizontal well in thick-layer heavy oil reservoirs. Geoenergy Science and Engineering, 2024, 241: 213108.

Wang, H. Modeling of multiple thermal fluid circulation in horizontal section of wellbores. Energy, 2023, 282: 128959.

Wang, Z., Du, H., Li, S., et al. Experimental study on gas-assisted cyclic steam stimulation under heavy-oil sandstone reservoir conditions: Effect of N_2/CO_2 ratio and foaming agent. Geoenergy Science and Engineering, 2023, 228: 211976.

Weng, J., Tan, Y., Wang, T., et al. Optimization and experimental study of flue gas-assisted SAGD process parameters for heavy oil thermal recovery. Fuel, 2025, 397: 135268.

Wu, Z., Vasantharajan, S., El-Mandouh, M., et al. Inflow performance of a cyclic-steam-stimulated horizontal well under the influence of gravity drainage. SPE Journal, 2011, 16(3): 494-502.

Wu, Z., Liu, H., Zhang, Z., et al. A novel model and sensitive analysis for productivity estimate of nitrogen assisted cyclic steam stimulation in a vertical well. International

Journal of Heat and Mass Transfer, 2018, 126: 391-400.

Yi, L., Hua, X., Guan, W., et al. Pilot project: Application of multi-component thermal fluid stimulation on shallow heavy oil reservoir in Kazakhstan. Paper SPE 204818 Presented at the SPE Middle East Oil & Gas Show and Conference, event canceled, 28 November-1 December, 2021.

Yan, X., Pang, Z., Liu, D., et al. The characteristics of steam chamber expanding and the EOR mechanisms of tridimensional steam flooding (TSF) in thick heavy oil reservoirs. Geoenergy Science and Engineering, 2025, 244: 213434.

Zhou, Y., Yao, C., Zhu, J., et al. Enhanced oil recovery in bottom-water heavy oil reservoirs with positive plugging-reverse displacement method: Based on 3D experiments and numerical simulation. Geoenergy Science and Engineering, 2025: 214118.

Zhang, Q., Liu, H., Kang, X., et al. An investigation of production performance by cyclic steam stimulation using horizontal well in heavy oil reservoirs. Energy, 2021, 218: 119500.

Zhu, Q., Jia, X., Li, B., et al. Mathematical modeling of foamy-oil flow in a cyclic solvent injection process. Journal of Petroleum Science and Engineering, 2022, 215: 110594.

Zhao, R., Wang, J., Men, Z., et al. Experimental investigation on cyclic steam stimulation assisted modified THAI to enhance oil recovery in steam-treated heavy oil. Energy, 2024, 307: 132533.

Zhao, D. W., Wang, J., Gates, I. D. Thermal recovery strategies for thin heavy oil reservoirs. Fuel, 2014, 117: 431-441.

Appendix A. Productivity model

The flow resistance in Eq. (8) can be represented by the expressions below, corresponding to the different stages of heated zone expansion:

$$R^1_{o,in} + R^1_{o,out} = R_{o,ins1} + R_{o,inh1} + R_{o,inc1} + R_{o,outc1} \tag{A1}$$

$$R^2_{o,in} + R^2_{o,out} = R_{o,ins2} + R_{o,inh2} + R_{o,outh2} + R_{o,outc2} \tag{A2}$$

$$R^3_{o,in} + R^3_{o,out} = R_{o,ins3} + R_{o,outs3} + R_{o,outh3} + R_{o,outc3} \tag{A3}$$

where

$$R_{o,\,ins1} = \frac{\mu_{os}}{2\pi \cdot L \cdot K \cdot K_{ros}} \left(\ln \frac{r_{s1}}{r_w} - \frac{r_{s1}^2}{2r_V^2} + S_k \right) \cdot B_o \tag{A4}$$

$$R_{o,\,inh1} = \frac{1}{2\pi \cdot L \cdot K} \int_{r_{s1}}^{r_{h1}} \frac{\mu_{oh}}{K_{roh}} \left(\frac{1}{r} - \frac{r}{r_V^2} \right) dr \cdot B_o \tag{A5}$$

$$R_{o,\,inc1} = \frac{\mu_{oc}}{2\pi \cdot L \cdot K \cdot K_{roc}} \left(\ln \frac{r_V}{r_{h1}} - \frac{1}{2} + \frac{r_{h1}^2}{2r_V^2} \right) \cdot B_o \tag{A6}$$

$$R_{o,\,outc1} = \frac{\mu_{oc}}{2\pi \cdot h \cdot K \cdot K_{roc}} \left(\ln \frac{r_e}{r_p} - \frac{3}{4} + \frac{r_p^2}{2r_e^2} \right) \cdot B_o \tag{A7}$$

$$R_{o,ins2} = \frac{\mu_{os}}{2\pi \cdot L \cdot K \cdot K_{ros}} \left(\ln \frac{r_{s2}}{r_w} - \frac{r_{s2}^2}{2r_V^2} + S_k \right) \cdot B_o \tag{A8}$$

$$R_{o,\,inh2} = \frac{1}{2\pi \cdot L \cdot K} \int_{r_{s2}}^{r_V} \frac{\mu_{oh}}{K_{roh}} \left(\frac{1}{r} - \frac{r}{r_V^2} \right) dr \cdot B_o \tag{A9}$$

$$R_{o,outh2} = \frac{1}{2\pi \cdot h \cdot K} \int_{r_p}^{r_{h2}} \frac{\mu_{oh}}{K_{roh}} \left(\frac{1}{r} - \frac{r}{r_e^2} \right) dr \cdot B_o \tag{A10}$$

$$R_{o,outc2} = \frac{\mu_{oc}}{2\pi \cdot h \cdot K \cdot K_{roc}} \left(\ln \frac{r_e}{r_{h2}} - \frac{3}{4} + \frac{r_{h2}^2}{2r_e^2} \right) \cdot B_o \tag{A11}$$

$$R_{o,ins3} = \frac{\mu_{os}}{2\pi \cdot L \cdot K \cdot K_{ros}} \left(\ln \frac{r_V}{r_w} - \frac{1}{2} + S_k \right) \cdot B_o \tag{A12}$$

$$R_{o,outs3} = \frac{\mu_{os}}{2\pi \cdot h \cdot K \cdot K_{ros}} \left(\ln \frac{r_{s3}}{r_p} - \frac{r_{s3}^2}{2r_e^2} + \frac{r_p^2}{2r_e^2} \right) \cdot B_o \tag{A13}$$

$$R_{o,outh3} = \frac{1}{2\pi \cdot h \cdot K} \int_{r_{s3}}^{r_{h3}} \frac{\mu_{oh}}{K_{roh}} \left(\frac{1}{r} - \frac{r}{r_e^2} \right) dr \cdot B_o \tag{A14}$$

$$R_{o,outc3} = \frac{\mu_{oc}}{2\pi \cdot h \cdot K \cdot K_{roc}} \left(\ln \frac{r_e}{r_{h3}} - \frac{3}{4} + \frac{r_{h3}^2}{2r_e^2} \right) \cdot B_o \tag{A15}$$

where $R_{o,ins}$, $R_{o,\,inh}$, and $R_{o,\,inc}$ are the oil phase flow resistances of SA, HA, and CA, respectively, within the vertical plane, (MPa·d)/m^3; $R_{o,\,outs}$, $R_{o,\,outh}$, and $R_{o,\,outc}$ are the oil phase flow resistances of SA, HA, and CA, respectively, within the horizontal plane, (MPa·d)/m^3; numerical superscript/subscript represents different phases of the heated zone expansion process; μ_{os}, μ_{oh}, and μ_{oc} are the oil viscosities in SA, HA and CA, respectively, mPa·s; K is the absolute permeability of the reservoir, 10^{-3} μm^2; K_{ros}, K_{roh}, and K_{roc} are the oil relative permeabilities in SA, HA and CA, respectively; h is the reservoir thickness, m; r_V is the outer boundary radius (half the reservoir thickness) within the vertical plane, m; r_p is the inner boundary radius (a quarter of the horizontal section length) within the horizontal plane, m; S_k is the skin factor; B_o is the oil formation volume factor, m^3/m^3.

Appendix B. Auxiliary equations

Appendix B.1 Average reservoir temperature

The multi-thermal fluid huff-n-puff process comprises three distinct stages: injection, soaking, and production. At the end of the injection phase, according to the model assumptions, the average temperature of the steam zone equals the injection temperature, while that of hot-water zone can be obtained from Eq. (B1):

$$T_{he} = \frac{\int_{r_s}^{r_h} T_h \cdot 2\pi r\, dr}{A_h - A_s} \tag{B1}$$

Considering heat conduction, the average temperatures of the steam zone and hot-water zone during the soaking process

are given, respectively, by Eqs. (B2) and (B3):

$$T_{savg} = T_i + (T_s - T_i)V_{rs} \tag{B2}$$

$$T_{havg} = T_i + (T_{he} - T_i)V_{rh} \tag{B3}$$

With the additional consideration of heat extraction by produced fluids, the average temperatures of the steam zone and hot-water zone during the production stage are given, respectively, by Eqs. (B4) and (B5):

$$T_{as} = T_i + (T_s - T_i)(V_{rs}(1 - O_s) - O_s) \tag{B4}$$

$$T_{ah} = T_i + (T_{he} - T_i)(V_{rh}(1 - O_h) - O_h) \tag{B5}$$

where T_{he} is the average temperature in HA at the end of the injection phase, °C; T_{savg} and T_{havg} are the average temperatures in SA and HA during the soaking phase, °C; V_{rs} and V_{rh} are the radial heat loss coefficients in SA and HA; T_{as} and T_{ah} are the average temperatures in SA and HA during the production stage, °C; O_s and O_h are the produced fluid heat loss correction factors in SA and HA.

Appendix B.2 Average reservoir pressure

Due to the ability of nitrogen in the non-condensable gas components to supplement formation pressure, the calculation of the average formation pressure at the end of the soaking period accounts for both the pressure change induced by steam injection and the pressure increase resulting from nitrogen injection, as shown in Eq. (B6):

$$P_{avg,s} = P_i + \frac{G_w \cdot B_w + G_n \cdot B_n}{N \cdot B_o \cdot C_e} + \frac{N_{os} \cdot (T_{savg} - T_i) \cdot \beta_e}{N \cdot C_e} + \frac{N_{oh} \cdot (T_{havg} - T_i) \cdot \beta_e}{N \cdot C_e} \tag{B6}$$

Considering pressure depletion due to fluid production, the average reservoir pressure during the production stage can be determined by Eq. (B7):

$$P_{avg,p} = P_{avg,s} - \frac{N_w B_w + N_o B_o}{N \cdot B_o \cdot C_e} - \frac{N_{os}(T_{savg} - T_{as}) \cdot \beta_e}{N \cdot C_e} - \frac{N_{oh}(T_{havg} - T_{ah}) \cdot \beta_e}{N \cdot C_e} \tag{B7}$$

where $P_{avg,s}$ is the average reservoir pressure at the end of the soaking phase, MPa; P_i is the original reservoir pressure, MPa; G_w and G_n are the injected volume of water and nitrogen under standard surface conditions, m^3; B_w and B_n are the formation volume factor of water and nitrogen, m^3/m^3; N, N_{os}, and N_{oh} are the original oil in place of the entire reservoir, the original oil in place of the steam zone, and the original oil in place of the hot-water zone, respectively, m^3; C_e is the total reservoir compressibility, MPa^{-1}; β_e is the reservoir thermal expansion coefficient, $°C^{-1}$; $P_{avg,p}$ is the average reservoir pressure during the production phase, MPa; N_o and N_w are the cumulative oil production and cumulative water production, m^3.

Appendix B.3 Average water saturation

According to the water phase mass conservation equation, the change in water saturation can be characterized as follows:

$$S_w = S_{wi}\frac{d_{wi}}{d_w} + \frac{G_w - N_w}{\phi \pi r_h^2 L} \tag{B8}$$

where S_w is the dynamic water saturation; S_{wi} is the original water saturation; d_{wi} is the initial density of water, kg/m^3; d_w is the dynamic water density, kg/m^3; ϕ is the porosity.

Appendix B.4 Relative permeability

In thermal recovery processes, relative permeability depends on both water saturation and temperature. Temperature primarily influences the relative permeability endpoints, specifically causing changes in irreducible water saturation and residual oil saturation, whereas the shape of the relative permeability curves remains consistent. For different combinations of temperature and water saturation, the oil relative permeability is given by Eq. (B9). Then, with the oil relative permeability curves at different temperatures (Fig. B1), the dynamics of oil relative permeability in the production process can be obtained. Similarly, the water relative permeability can be determined:

$$K_{ro}(S_{wn}) = \frac{S_{wn} - S_{w,i}}{S_{w,k} - S_{w,i}} K_{ro}(S_{w,k}) + \frac{S_{w,k} - S_{wn}}{S_{w,k} - S_{w,i}} K_{ro}(S_{w,i}) \tag{B9}$$

where

$$S_{wn} = S_w - \frac{T - T_1}{T_2 - T_1}(S_{orw1} - S_{orw2}) \tag{B10}$$

where K_{ro} is the oil relative permeability; S_{wn} is the corrected water saturation value accounting for the effect of temperature on relative permeability endpoints; $S_{w,i}$ and $S_{w,k}$ are different water saturation values; T, T_1, and T_2 are different temperatures, °C; S_{orw1} represents the residual oil saturation at temperature T_1; S_{orw2} represents the residual oil saturation at temperature T_2.

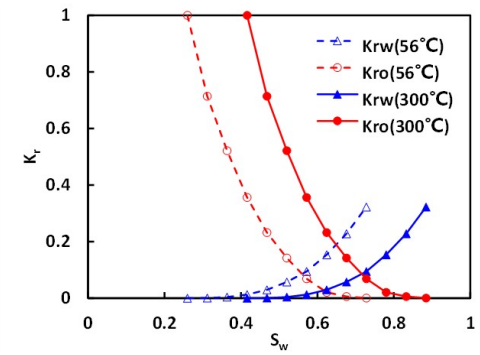

Fig. B1. Oil-water relative permeability curves for M Reservoir at different temperatures.

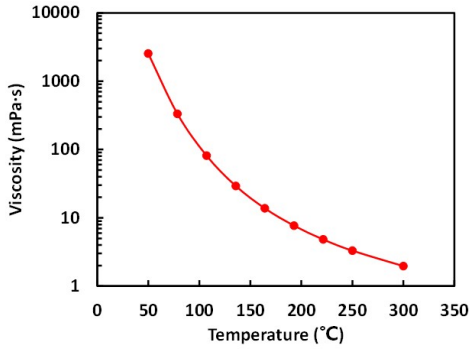

Fig. B2. Viscosity-temperature curve of crude oil for M Reservoir.

Appendix B.5 Oil viscosity

The relationship between heavy oil viscosity and temperature is typically expressed as Eq. (B11), thus, based on the viscosity-temperature data points in Fig. B2, the viscosity of heavy oil at any given temperature can be calculated:

$$\lg\lg \mu_{ot} = C - D\lg T \tag{B11}$$

Accounting for the viscosity reduction effect due to carbon dioxide dissolution, the viscosity of the heavy oil-carbon dioxide composite system can be determined by the following equation (Hou et al., 2016; Jiang et al., 2024):

$$\ln \mu_o = (1 - x_i)\ln \mu_{ot} + x_i(\ln \mu_c + m - n\ln T) \tag{B12}$$

where μ_{ot} is the oil viscosity, mPa·s; C and D are constants; μ_o is the viscosity of heavy oil-carbon dioxide composite system, mPa·s; x_i is the mole fraction of carbon dioxide in the heavy oil-carbon dioxide composite system; μ_c is the carbon dioxide viscosity, mPa·s; m and n are constants.

Appendix B.6 Threshold pressure gradient

A mobility-dependent relationship is employed to characterize the threshold pressure gradient of heavy oil, as shown in Eq. (B13):

$$G = 0.0389\left(\frac{K}{\mu_o}\right)^{-0.983} \tag{B13}$$

Appendix B.7 Residual heat from previous cycle

To determine the multi-cycle productivity, the influence of residual heat from previous cycles on the heated zone must be considered. Specifically, Eqs. (B14) and (B15) are employed to calculate the residual heat in the steam zone and hot-water zone, respectively:

$$E_{rs} = \pi r_s^2 LM_R(T_{as} - T_i) \tag{B14}$$

$$E_{rh} = \pi\left(r_h^2 - r_s^2\right)LM_R(T_{ah} - T_i) \tag{B15}$$

where E_{rs} is the residual heat in SA, kJ; E_{rh} is the residual heat in HA, kJ.